NZGS SYMPOSIUM 2020
Good grounds for the future
15–17 October 2020 · Dunedin · New Zealand

Response of gravel-rubber mixtures under direct shear testing: experimental and DEM numerical investigations

K. Chew
Beca Infrastructure & University of Canterbury, Christchurch.

G. Chiaro & A. Tasalloti
Department of Civil and Natural Resource Engineering, University of Canterbury, Christchurch.

J.S. Vinod & K. Allulakshmi
School of Civil, Mining & Environmental Engineering, University of Wollongong, Australia.

ABSTRACT

This paper presents the results from direct shear testing of gravel-rubber mixtures through laboratory experiments and numerical simulations with discrete element method (DEM). Mixtures with volumetric proportions of 0%, 10%, 25%, 40% and 100% granulated rubber were tested using a conventional, medium-sized direct shear apparatus under three normal stresses: 30, 60 and 100 kPa. Experimental results show a decrease in shear strength, greater strain at peak shear stress and less dilative behaviour with increasing rubber content. A selection of experimental results were used to calibrate the DEM model to examine the macro- and micro-responses of the mixtures. Good agreement was attained between the simulation and laboratory results under different normal stresses. This simulation exercise demonstrates that DEM is a suitable tool to describe the mechanical behaviour of mixtures made of hard-gravel and soft-rubber particles under direct shear loads without overly complex input parameters.

1 INTRODUCTION

In 2015, less than a quarter of the four million waste tyres were recycled with most ending up in landfills or dumped in stockpiles around the country (Minister of the Environment, 2015). This issue plagues several countries globally, with many placing strict regulations on deposing waste tyres and implementing recycle and reuse methods. In New Zealand, the “Eco-rubber geotechnical seismic-isolation (ERGSI) foundation systems” project aims to help address this problem using gravel-recycled tyre rubber mixtures to improve the seismic performance of medium-density low-rise residential buildings, with the ERGSI providing an appreciable level of base isolation and energy dissipation during ground shaking. This study is part of a multi-disciplinary research project being undertaken by researchers of the University of Canterbury and the Institute of Environmental Science and Research (ESR) Ltd. (Chiaro et al. 2019; Banasiak et al. 2019; Hernandez et al. 2020).

The incorporation of rubber in granular soils has been increasingly common since the 1990s. Rubber's low unit weight has seen its use as a lightweight backfill material for retaining walls and embankments (Lee et al. 1999; Humphrey & Manion 1992). In seismic applications, energy dissipative effects of rubber have been studied as a countermeasure against liquefaction (Hazarika et al. 2020; Anastasiadis et al. 2012) and as a geotechnical isolation system (Tsang 2008).

To date, previous studies of soil-rubber mixtures have predominantly focused on sand-rubber mixtures, SRM (e.g. Mashiri et al. 2015; Valdes & Evans 2008; Hazarika et al. 2008; Lee et al. 2014). However, the use of gravel rather than sand in soil-rubber mixtures has been recommended (Hazarika & Adbullah 2016) to avoid inherent segregation of binary mixtures made of large and small particles (Lee & Santamarina, 2008). Yet, studies on gravel-rubber mixtures are very limited (e.g. Signes et al. 2013, Pasha et al. 2018).

With the advancement of computing power over the last few decades, many researchers have attempted to use numerical simulations to study the microscopic behaviours of soil mixtures. DEM has been widely used in recent years to study the behaviour of geomaterial such as SRM and railway ballast subjected to direct shear testing, compression and triaxial tests (e.g. Lopera-Perez et al. 2018; Asadi et al. 2018; Gong et al. 2019; Wang et al. 2018; Lim and McDowell 2005; Indraratna et al. 2014).

In this study, through the use of experimental and numerical simulations, the behaviour of gravel-rubber mixtures under direct shear has been studied with consideration of different rubber content and normal stresses. Emphasis is placed on developing a tool to complement laboratory experiments to provide a better understanding of the behaviour of these mixtures using insights from microscopic level responses.

2 EXPERIMENTS

2.1 Material and Testing Procedures

The direct shear apparatus used in this study consist of a 100 mm by 100 mm wide metal square box with a height of 53 mm divided in two halves (refer to Figure 4 for details). The tested materials consisted of a uniformly-graded granulated tyre rubber (specific gravity $G_{s,R}$ = 1.15; mean particle size $D_{50,R}$ = 4 mm) and a uniformly-graded rounded gravel (specific gravity $G_{s,G}$ = 2.71; mean particle size $D_{50,G}$ = 6mm). The aspect ratio ($D_{50,G}/D_{50,R}$) of the mixtures was approximately 1.5. The particle size distribution of the gravel and rubber alongside a specimen of the geomaterial tested are shown in Figure 1.

The direct shear tests were conducted in accordance with ASTM D3080 under normal stresses of 30, 60 and 100 kPa. Mixtures with varying volumetric proportions of rubber crumbs (i.e. 10%, 25% and 40% rubber content) were prepared by mixing dry gravel and rubber particles. The test specimens were placed into the shear box in four roughly equal layers, with a small compacting force applied at each layer (refer to under-compaction method by Ladd, 1978) to ensure the specimens were properly packed inside the box while avoiding segregation. The relative density of all specimens before applying any vertical stress was 50%.

The displacement-controlled procedure was used to shear the specimen at a rate of 1mm/min to a maximum shear displacement of 16 mm. Shear stress, vertical displacement, and horizontal displacement were recorded throughout the entire test. A summary of the direct shear tests carried out on various gravel-rubber mixtures is reported in Table 1.

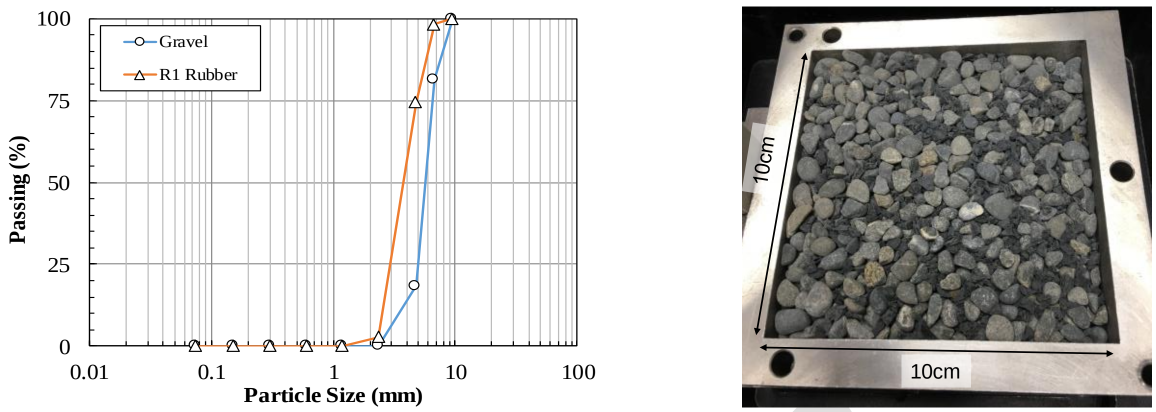

(a) **(b)**

Figure 1. (a) Particle size distribution for the sourced gravel (G) and granulated rubber (R1); and (b) photograph of a specimen of test materials used in this study.

Table 1: Properties of the gravel rubber mixtures.

Mixture ID	Volumetric rubber content, *VRC* (%)	Specific Gravity, G_s	(Initial) Void ratio, *e*
G100-R0	0	2.71	0.63
G90-R10	10	2.51	0.65
G75-R25	25	2.33	0.70
G60-R40	40	2.09	0.74
G0-R100	100	1.15	1.01

3 DISCRETE ELEMENT METHOD

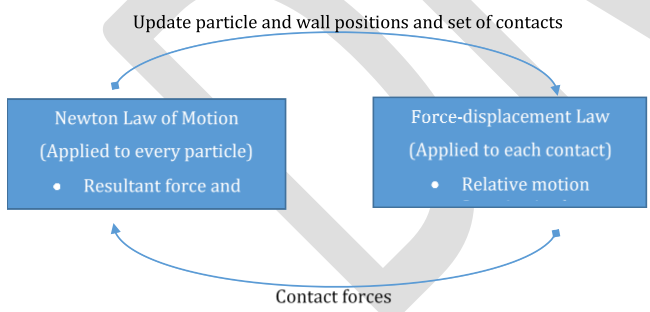

Figure 2. Description of a calculation cycle in PFC3D (Itasca Consulting Group 2019).

The use of discrete elements methods (DEM) to model distinct particles was originally proposed by Cundall and Strack (1979) and is now widely used where discrete nature of systems exist. It has application across several engineering fields from the study of jointed rock masses, rock falls to the flow of bulk materials.

In this study, the commercially available software by Itasca Consulting Group - Particle Flow Code 3-dimensional (PFC3D) is used. PFC3D is based on the discrete numerical model originally proposed by Cundall and Strack (1979) which uses an explicit numerical scheme to monitor the interaction of particles individually and its corresponding contacts with neighbouring particles. This DEM framework utilises brief states of equilibrium to numerically describe a dynamic behaviour. It assumes that the velocities and accelerations are constant within each time step and that time steps are infinitesimal such that disturbances on a particle assemble does not propagate beyond its immediate neighbours (Cundall & Strack 1979). The calculation cycle in PFC3D is illustrated in Figure 2 and is fundamentally based on Newton’s second law and a typical force-displacement law.

In this context, rigid-hard gravels and soft granulated rubber are modelled in DEM as individual and unbonded particles where the physical properties of each particle are defined. Input parameters for each particle include: shape, size, stiffness, surface friction and an interaction relationship (i.e. contact law) to describe the behaviour of particles within the system. Spring and dashpot forces as a function of the particle overlap are typically used to describe the interaction between model components at its contacts (Figure 3). In the model, particle slip occurs when the tangential forces exceed the Coulomb limit defined by the friction coefficient, μ (Itasca, 2019).

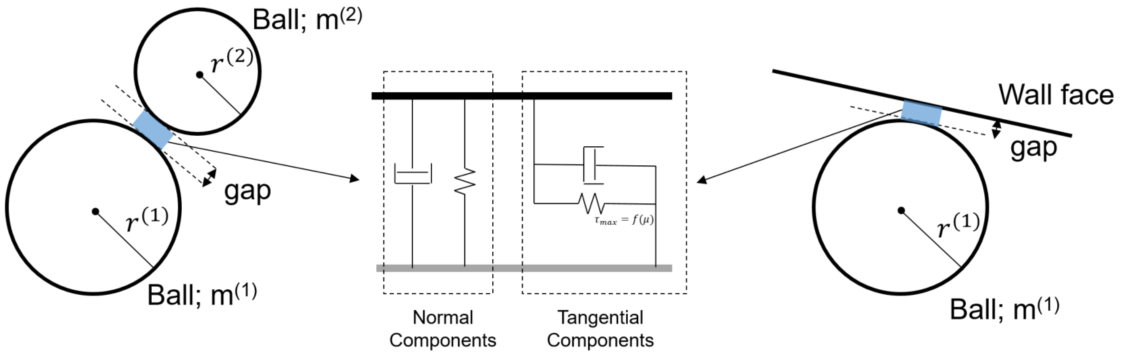

Figure 3. Model component definitions and interactions for a linear contact model, where m and r denote mass and radius of ball respectively (Itasca, 2019).

3.1 Model Parameters and Setup

Figure 4 shows how the corresponding components of a direct shear apparatus are represented in the DEM model. The model consists of walls akin to boundaries and spherical particles grouped together to form clumps. The box is sheared by moving the bottom half of the box at a constant deformation rate. To reduce computation time, the samples were sheared at a rate of 0.01m/s found by limiting the inertia number, $I < 1e^{-3}$ proposed by Lopera-Perez at al. (2016) to satisfy quasi-static conditions.

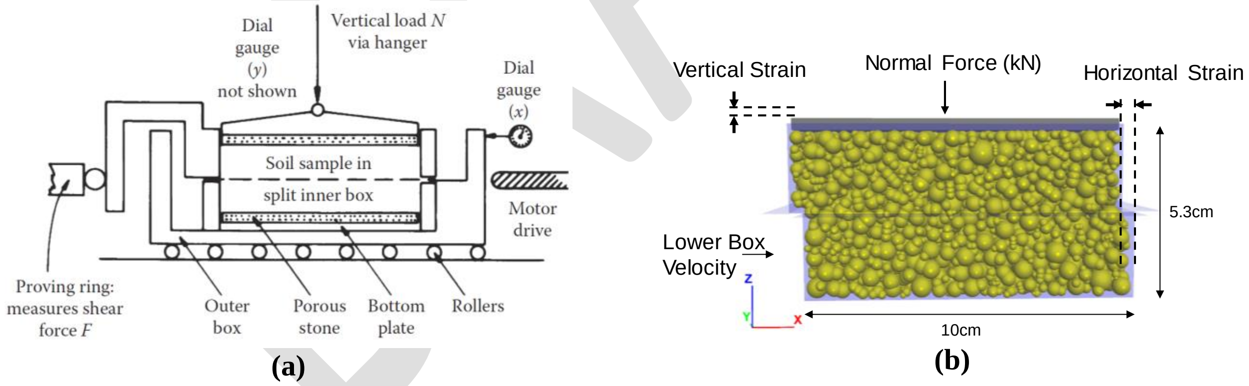

Figure 4. (a) Schematic illustration of direct shear apparatus (Powrie 2014); (b) DEM model of the direct shear test in this study.

The inertia number is defined as $I = \dot{\varepsilon} d \sqrt{\rho / p'}$, where $\dot{\varepsilon}$ is the strain rate, d is the average particle size, ρ is the particle density and p' is the mean effective stress which is assumed to be the normal stress applied. This results in an average computational time of 2 hours per test using a 48 CPU (central processing unit) cluster and a time step in the order of 10^{-6} seconds.

The shear force is measured by taking the increments in the sum of forces in the shearing direction applied by the particles onto the walls of the top half of the box during shearing (Indraratna et al. 2014; Zhang & Thornton 2007).

As shown in Figure 5, simple shapes were used to represent the gravel and rubber particles. Conglomerate of balls (clumps) were used to represent the rounded gravels and rubber crumbs respectively. The gravel and rubber particles were determined from the particle size distribution in Figure 1(a) and placed randomly with particle-to-particle overlaps in the shear box to achieve a target mass corresponding to 50% relative density.

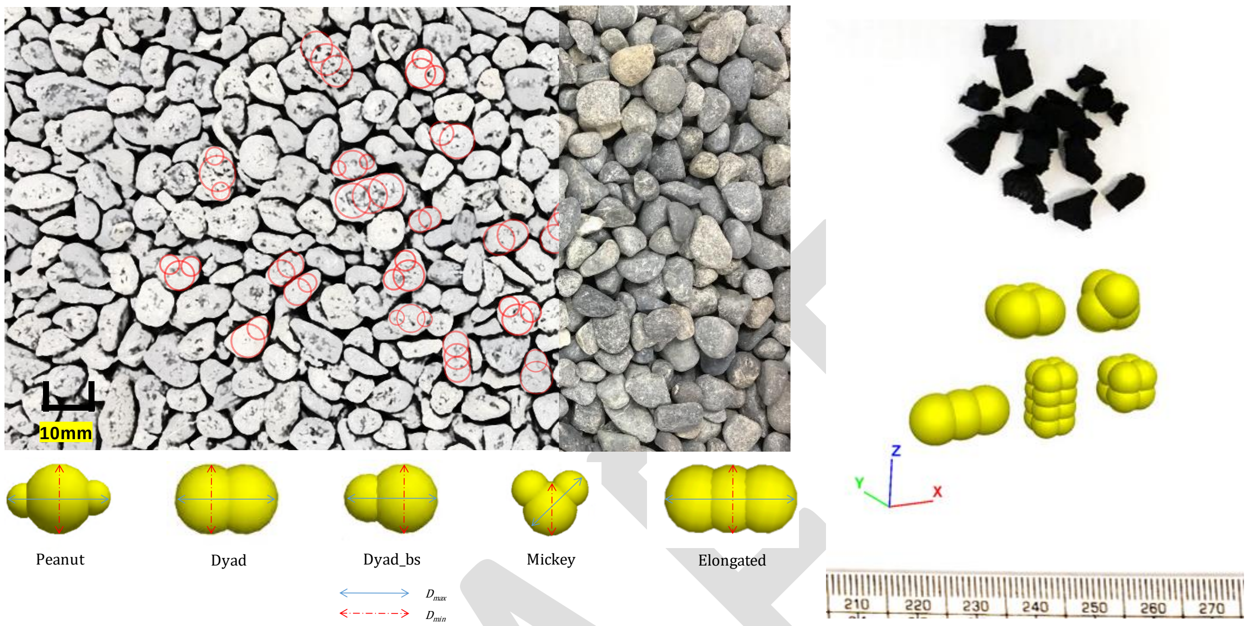

Figure 5. Simple shapes used in this study to approximate gravel (G) and rubber (R) particle geometry.

A combination of parameters calibrated from test results and adopted from the literature have been used in this simulation. The Hertz-Mindlin (Mindlin & Deresiewicz, 1953) contact law was found to be the most appropriate to produce good results at different normal stresses. These numerical parameters are summarised in Table 2.

Table 2: Numerical parameters for gravel, rubber and shear box.

Parameter	**Gravel**	**Rubber**	**Shear box**
Particle Density, ρ (kg/m^3)	2710[(1)]	1150[(1)]	-
Shear modulus, G (MPa)	90 [(2)]	6 [(3)]	80,000 [(4)]
Poisson's Ratio, υ	0.25 [(2)]	0.49	0.30 [(4)]
Coefficient of Friction *	0.80	0.30	0.70 for wall-gravel 0.20 for wall-rubber

[(1)] Tasalloti et al., 2020; [(2)] determined from bender element test of G100-R0; [(3)] Lopera-Perez at al., 2018; [(4)] Beer et al., 2015.

* derived from calibration process

4 RESULTS AND DISCUSSIONS

4.1 Pure Gravel and Pure Rubber

The shear stress versus vertical displacement and horizontal displacement versus vertical displacement plots, experimentally and numerically obtained for pure gravel and rubber at 30, 60 and 100 kPa normal stresses, are shown in Figure 6.

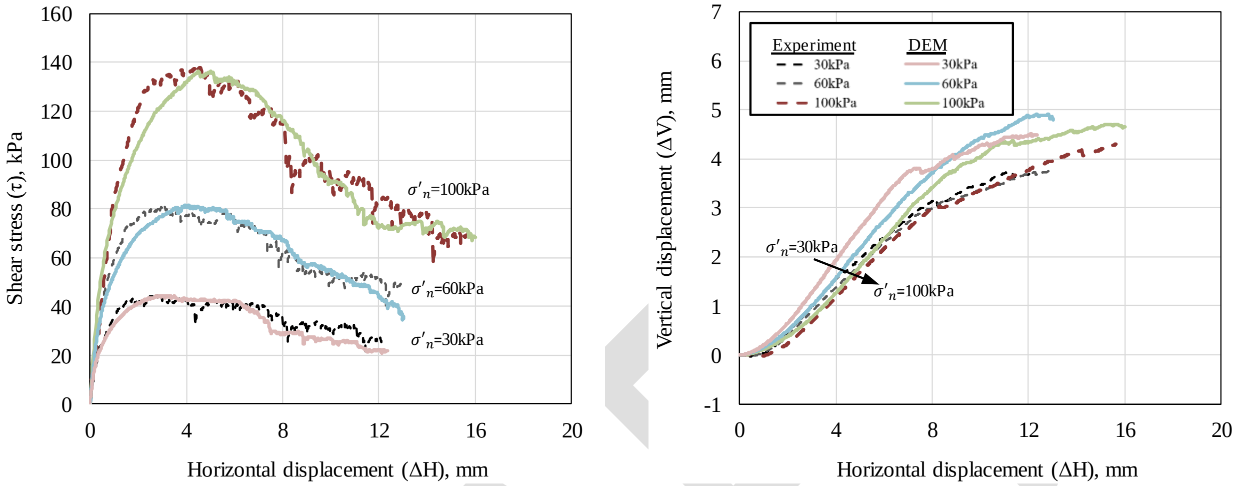

(a) G100

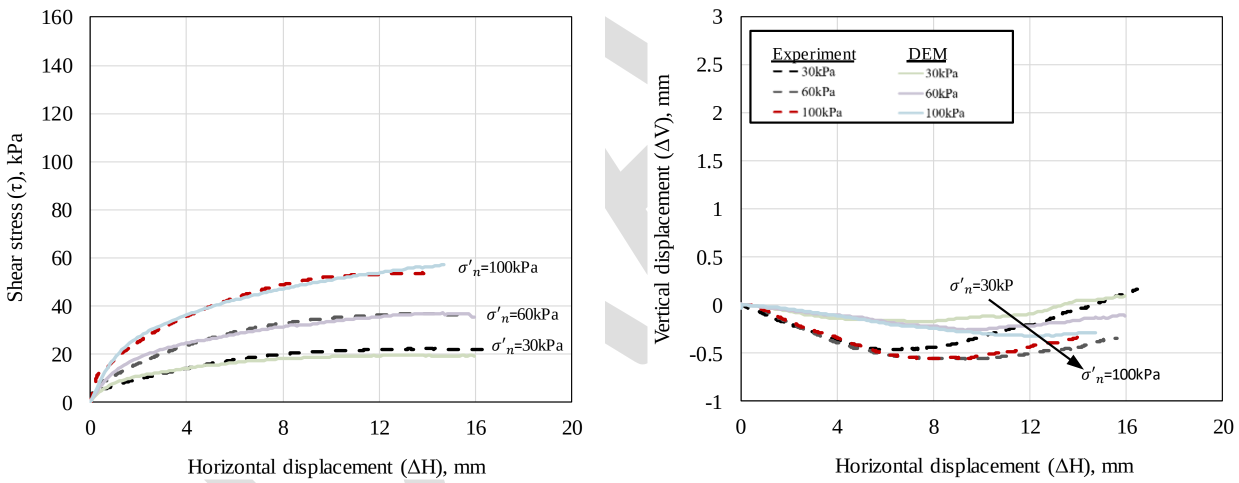

(b) R100

Figure 6. Experimental and numerical results of direct shear test on pure gravel and rubber

4.1.1 Experimental

There are several key differences between the behaviour of the pure gravel and pure rubber samples under direct shear: (1) a clear peak is followed by strain softening as evident in the shear stress curve for pure gravel, which is absent in pure rubber; (2) pure gravel exhibit predominantly dilative behaviour during shearing while that of pure rubber is predominantly contractive; and (3) the maximum shear stress measured during shearing in gravel is significantly greater that rubber under the same normal stress.

4.1.2 Numerical model

Figure 6(a) also show the comparison between the experimental data and the DEM numerical simulations for 100% rounded gravel under three different normal stresses and 50% relative density. The DEM results show good agreement with the experimental data in terms of trends, rate of dilation and total vertical displacements.

At large deformation levels, the simulated shear stress is ±5 kPa dissimilar to that measured in laboratory experiments, while the total vertical displacement predicted is slightly overestimated,differing by less than 1 mm.

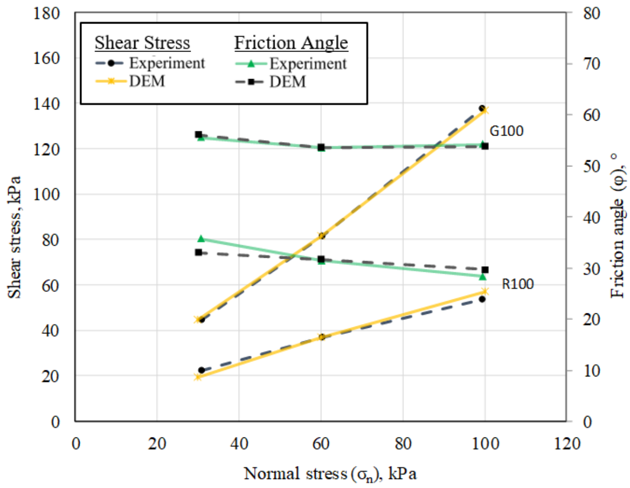

Figure 7. Comparison of friction angle and shear stress results at failure/peak

In the case of pure rubber, a good agreement is attained between the shear stress–shear displacement relationships experimentally obtained and the corresponding DEM simulations. As shown in Figure 6(b), the model prediction for the vertical-horizontal displacement plots is still able to capture the overall qualitative trends. For example, contractive response followed by dilative behaviour after the maximum compression and the measured vertical displacement typical differ by less than 0.4 mm. Some small quantitative differences can also observed. For instance, the rate of contraction is greater in the experimental results and the numerical model achieves the maximum contraction at a large displacement as compared to the experiment.

In terms of predicting the strength characteristics of gravel and rubber (e.g. peak shear stress and peak friction angle), the DEM model's results show a good agreement with experimental results as shown in Figure 7.

4.1.3 Micro-responses

Figure 8 illustrates the rotation in the major principle stress in the DEM sample during shearing, which is characteristic of direct shear testing and is not easily measureable in laboratory experiments.

By measuring the average normal force components at each contact in the system, the distribution of average normal forces can be obtained as shown in Figure 8. Before shearing, the sample is inherently anisotropic with the direction of maximum average normal force, θ_n, orientated 90 degrees to the horizontal as a result of the non-isotropic conditions of a direct shear apparatus. During shearing, θ_n reduces to 30 degrees at peak stress (4mm displacement) and increases to 35-45 degrees at post-peak (>10mm displacement). Note that θ_n may not necessarily be in line with the major principle stress direction (Rothenburg & Bathurst 1989), but may be used as a proxy.

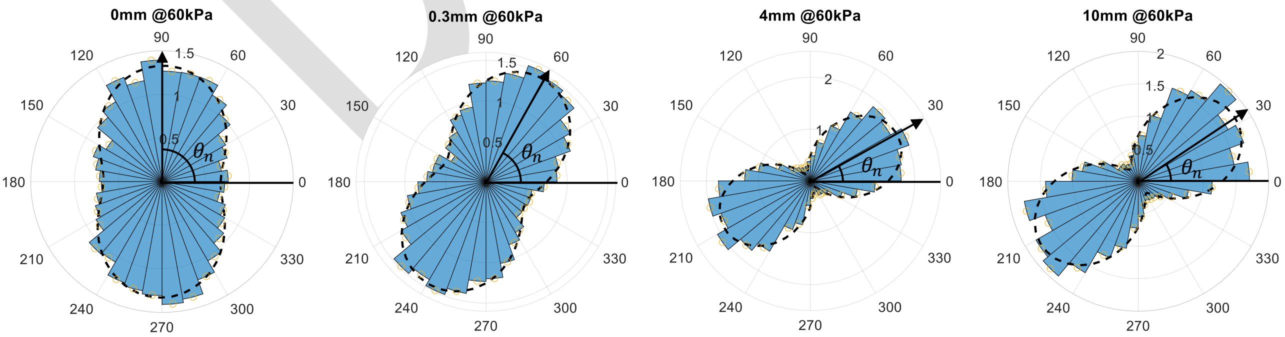

Figure 8. Polar histogram of average normal forces in the DEM sample at different deformation level for G100 under 60 kPa normal stress.

4.2 Gravel-rubber Mixtures

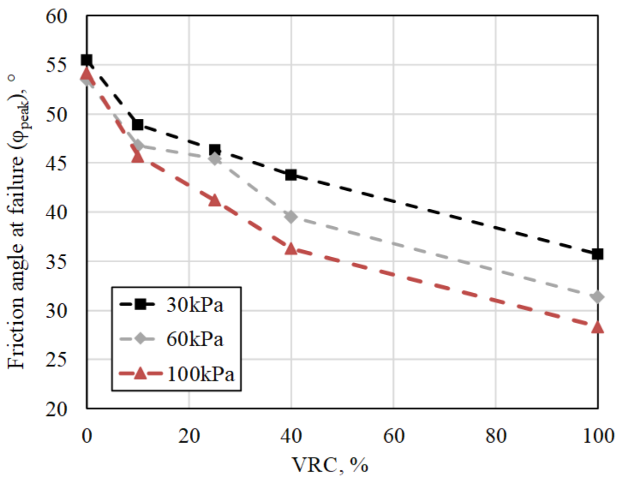

Figure 9. Friction angle at failure under different VRC.

The effects of different volumetric rubber content on the shear stress and vertical displacement under 30, 60 and 100 kPa normal stress were also examined in this study. Experimental results show that the peak shear stress decreases with increasing rubber content while the vertical displacement decreases with increasing rubber content (Tasalloti et al., 2020). The experimental results summarised in Figure 8 show that the inclusion of rubber causes a reduction in the friction angle (at peak or large displacement) for all normal stress levels.

It is evident that the inclusion of rubber causes a reduction in strength of the soil mixture. However, the peak friction angle measured for Volumetric rubber content (*VRC) of* 40% or less were typically 35 degrees or greater, which is in the order of what it typically recommended for structural fills in practice (Chiaro et al. 2015).

The behaviour of gravel-rubber mixtures can be differentiated by three categories: (stiff) gravel-dominant, intermediate and (soft) rubber-dominant behaviours. Based on the experimental results, gravel-dominant could be inferred for *VRC* < 10% where the material behaviour is characterised by an initially stiff response followed by a softening post-peak dilative response; rubber-dominant could be assumed for *VRC* > 40% where the initial response is much less stiff and the material showing a strain-hardening with contraction behaviour up to large displacement; in between intermediate behaviour could be assumed for 10%<*VRC*<40%.

4.2.1 Numerical model

Although specific simulation results are not reported in this paper, initial numerical results indicate that the gravel-rubber DEM model are able to capture the key characteristics and strength of the tested specimens under direct shear. In this context, the calibrated gravel and rubber models have been combined to study the prediction capabilities for gravel-rubber mixtures using DEM. Numerical results from mixtures of different volumetric rubber content will be published elsewhere in due course.

5 CONCLUSIONS

In this paper, the results of laboratory and numerical simulations of direct shear tests carried out on gravel-rubber mixtures, with volumetric rubber content *VRC* = 0, 10, 25, 40 and 100%, were presented. The experimental results showed a decrease in shear strength, greater strain at peak shear stress and less dilative behaviour with increasing rubber content. The numerical investigation was carried out by developing a direct shear box model for hard-grain gravel and soft-particle rubber materials in the DEM software PFC3D. With the use of simple shapes to approximate particle geometry, inputs from measured physical properties of gravel and rubber, and a rigorous calibration process, the DEM model results show good agreement with the experimental results and are able to capture key characteristics of the mechanical behaviour of both gravel and rubber under direct shear load (e.g. peak shear stress, peak friction angle and dilative/contractive behaviours). This model will be further advanced to examine the complex behaviour of gravel-rubber mixtures made of hard and soft particles from a microscopic and granular mechanics points of view, which are not easily measureable in physical laboratory experiments.

ACKNOWLEDGEMENTS

This study was funded by the Ministry of Business, Innovation and Employment of New Zealand (MBIE Smart Ideas Research Grant No. 56289). A special thank you goes to the University of Canterbury IT staff (Paul Strange) for setting up the computation engine.

REFERENCES

Anastasiadis, A., Senetakis, K. & Pitilakis, K. 2012. Small-Strain Shear Modulus and Damping Ratio of Sand-Rubber and Gravel-Rubber Mixtures. *Geotechnical and Geological Engineering*. Vol 30(2): 363-382.

ASTM International. 2011. *D3038: Standard Test Method for Direct Shear Test of Soils under Consolidated Drained Conditions*. American Society for Testing and Materials.

Banasiak, L.J., Chiaro, G., Palermo, A. & Granello, G. 2019. Recycling of end-of-life tyres in civil engineering applications: environmental implications. *WasteMINZ 2019 Conference*, Hamilton, New Zealand.

Beer, F.P., Johnston, E.R., DeWolf, J.T. & Mazurek, D.F. 2015. *Mechanics of materials. Seventh in SI units*. New York: McGraw-Hill Education.

Chiaro, G., Indraratna, B., Tasalloti, S.M.A. & Rujikiatkamjorn, C. 2015. Optimisation of coal wash–slag blend as a structural fill. *Ground Improvement.* Vol 168(1): 33-44.

Chiaro, G., Palermo, A., Granello, G., Tasalloti, A., Stratford, C. & Banasiak, L.J. 2019. Eco-rubber seismic-isolation foundation systems: a cost-effective way to build resilience. *Proc. 2019 Pacific Conference on Earthquake Engineering*, 4-6 April, Auckland, New Zealand, pp. 8.

Cundall, P.A. & Strack, O.D.L. 1979. A Discrete Numerical Model for Granular Assemblies. *Géotechnique*, Vol 29(1): 47-65.

Evans, T.M. & Valdes, J.R. 2008. Sand-rubber mixtures: Experiments and numerical simulations. *Canadian Geotechnical Journal*. Vol 45(4): 588-595.

Gong. L., Nie. L., Xu. Y., Wang. H., Zhang. T., Du, C., et al. 2019. Discrete element modelling of the mechanical behaviour of a sand-rubber mixture containing large rubber particles. *Construction and Building Materials*. Vol 205: 574-585.

Hazarika, H. & Abdullah, A. 2016. Improvement effects of two and three dimensional geosynthetics used in liquefaction countermeasures. *Japan Geotechnical Society Special Publication*, Vol 2(68): 2336–2341.

Hazarika, H., Pasha, S.M.K., Ishibashi, I., Yoshimoto, N., Kinoshita, T., Endo, S., et al. 2020. Tire-chip reinforced foundation as liquefaction countermeasure for residential buildings. *Soils and Foundations*.

Hazarika, H., Yasuhara, K., Karmokar, A.K. & Mitarai, Y. 2008. Shaking table test on liquefaction prevention using tire chips and sand mixture. *Proceedings of the International Workshop on Scrap Tire Derived Geomaterials - Opportunities and Challenges*. 215-222. Japan.

Hernandez, E., Palermo, A., Granello, G., Chiaro, G. & Banasiak, L.J. 2020. Eco-rubber seismic-isolation foundation system, a sustainable solution for the New Zealand context. *Structural Engineering International*. Vol 3(2): 192-200.

Hidalgo-Signes, C, Martínez-Fernández, P., Medel-Perallón, E., et al. 2015. Characterisation of an unbound granular mixture with waste tyre rubber for subballast layers. *Materials and Structures*. Vol 48(12): 3847-3861.

Humphrey, D.N. & Manion, W.P. 1992. Properties of tire chips for lightweight fill. *Grouting, Soil Improvement and Geosynthetics*. ASCE.

Indraratna, B., Ngo, N.T., Rujikiatkamjorn, C. & Vinod, J.S. 2014. Behavior of Fresh and Fouled Railway Ballast Subjected to Direct Shear Testing: Discrete Element Simulation. *International Journal of Geomechanics*. Vol 14(1): 34-44.

Itasca Consulting Group. 2019. PFC3D: Particle Flow Code in Three Dimensions, version 6.00.15.

Ladd, R. 1978. Preparing Test Specimens Using Undercompaction. *Geotechnical Testing Journal.* Vol 1(1): 16-23.

Lee, C., Shin, H. & Lee, J. 2014. Behavior of sand–rubber particle mixtures: experimental observations and numerical simulations. *International Journal for Numerical and Analytical Methods in Geomechanics*. Vol 38(16): 1651-1663.

Lee, J.H., Salgado, R., Bernal, A. & Lovell, C.W. 1999. Shredded Tires and Rubber-Sand as Lightweight Backfill. *Journal of Geotechnical and Geoenvironmental Engineering*. Vol 125(2): 132-141.

Lee, J.S., Doods, J. & Santamarina, J.C. 2007. Behavior of rigid-soft particle mixtures. *Journal of Material in Civil Engineering*, Vol 19(2): 179-184.

Lim, W.L. & McDowell, G.R. 2005. Discrete element modelling of railway ballast. *Granular Matter*. Vol 7(1): 19-29.

Lopera-Perez, J.C., Kwok, C.Y. & Senetakis, K. 2018. Effect of rubber content on the unstable behaviour of sand–rubber mixtures under static loading: a micro-mechanical study. *Géotechnique*. Vol 68(7): 561-574.

Lopera-Perez, J.C., Kwok, C.Y., O'Sullivan, C., Huang, X. & Hanley, K.J. 2016. Assessing the quasi-static conditions for shearing in granular media within the critical state soil mechanics framework. *Soils and Foundations*, Vol 56(1): 152-159.

Mashiri, M.S., Vinod, J.S., Sheikh, M.N. & Tsang, H. 2015. Shear strength and dilatancy behaviour of sand–tyre chip mixtures. *Soils and Foundations*. Vol 55(3): 517-528.

Mindlin, R.D. & Deresiewicz, H. 1953. Elastic Spheres in Contact under Varying Oblique Forces. Journal of Applied. Mechanics. Vol 20: 327-344.

Ministry for the Environment. 2015. Waste tyres economic research. Report 3, May 2015, pp. 87.

Pasha, S.M.K., Hazarika, H. & Yoshimoto, N. 2019. Physical and mechanical properties of Gravel-Tire Chips Mixture (GTCM). *Geosynthetics International*. Vol 26(1): 92-110.

Powrie, W. 2014. *Soil mechanics: concepts and applications. 3rd ed*. Boca Raton, Florida: CRC Press/Taylor & Francis.

Rothenburg, L. & Bathurst, R.J. 1989. Analytical study of induced anisotropy in idealised granular material. *Géotechnique*, Vol 39(4): 601-614.

Tasolloti, A., Chiaro, G., Palermo, A. & Banasiak, L. 2020. Effect of Rubber Crumbs Volumetric Content on the Shear Strength of Gravelly Soils in Direct Shear Apparatus. *Geo-Congress 2020*, 25-28 February, Minnesota, USA.

Tsang, H. 2008. Seismic isolation by rubber–soil mixtures for developing countries. *Earthquake Engineering & Structural Dynamics*. Vol 37(2): 283-303.

Wang, C., Deng, A. & Taheri, A. 2018. Three-dimensional discrete element modelling of direct shear test for granular rubber–sand. *Computers and Geotechnics*. Vol 97: 204-216.

Zhang, L. & Thornton, C. 2007. A numerical examination of the direct shear test. *Geotechnique*. Vol 57(4): 343-354.